Published in final edited form as:
Radiat Res. 2013 March ; 179(3): 343–351. doi:10.1667/RR2811.1.

Assessment of the Changes in 9L and C6 Glioma pO_2 by EPR Oximetry as a Prognostic Indicator of Differential Response to Radiotherapy

Huagang Hou[a,d], **Sriram P. Mupparaju**[a], **Jean P. Lariviere**[a,d], **Sassan Hodge**[c], **Jiang Gui**[b,d], **Harold M. Swartz**[a,d], and **Nadeem Khan**[a,d,1]

[a] EPR Center for Viable Systems, Department of Radiology, Geisel School of Medicine, Hanover, New Hampshire

[b] Community and Family Medicine, Geisel School of Medicine, Hanover, New Hampshire

[c] Department of Surgery, Dartmouth-Hitchcock Medical Center, Lebanon, New Hampshire

[d] Norris Cotton Cancer Center, Dartmouth-Hitchcock Medical Center, Lebanon, New Hampshire

Abstract

Tumor hypoxia impedes the outcome of radiotherapy. As the extent of hypoxia in solid tumors varies during the course of radiotherapy, methods that can provide repeated assessment of tumor pO_2 such as EPR oximetry may enhance the efficacy of radiotherapy by scheduling irradiations when the tumors are oxygenated. The repeated measurements of tumor pO_2 may also identify responders, and thereby facilitate the design of better treatment plans for nonresponding tumors. We have investigated the temporal changes in the ectopic 9L and C6 glioma pO_2 irradiated with single radiation doses less than 10 Gy by EPR oximetry. The 9L and C6 tumors were hypoxic with pO_2 of approximately 5–9 mmHg. The pO_2 of C6 tumors increased significantly with irradiation of 4.8–9.3 Gy. However, no change in the 9L tumor pO_2 was observed. The irradiation of the oxygenated C6 tumors with a second dose of 4.8 Gy resulted in a significant delay in growth compared to hypoxic and 2 Gy × 5 treatment groups. The C6 tumors with an increase in pO_2 of greater than 50% from the baseline of irradiation with 4.8 Gy (responders) had a significant tumor growth delay compared to nonresponders. These results indicate that the ectopic 9L and C6 tumors responded differently to radiotherapy. We propose that the repeated measurement of the oxygen levels in the tumors during radiotherapy can be used to identify responders and to design tumor oxygen guided treatment plans to improve the outcome.

INTRODUCTION

The imbalance between oxygen supply and consumption often leads to hypoxia in solid tumors, which is believed to compromise the efficacy of radiotherapy and enhance aggressive tumor behavior and metastases (1–5). Consequently, a significant increase in therapeutic outcome may be achieved if tumor hypoxia is minimized by improving the levels of oxygen in solid tumors. Preclinical and clinical investigations using pO_2 histograph and assays for hypoxic fractions have shown a substantial change in tumor oxygen after single dose (6, 7) or fractionated radiotherapy (8–12). While some useful information has been obtained in human gliomas by using oxygen electrodes or a fiber-optic probe (13, 14),

[1]Address for correspondence: EPR Center for Viable Systems, 716 Vail, Geisel School of Medicine, Hanover, NH 03755; Nadeem.Khan@Dartmouth.edu..

repeated measurements to assess the time course of the changes in glioma oxygen are not feasible by these methods, because they involve a significant degree of invasiveness, and cannot be used for repeated assessments of tumor pO_2 (15).

Several preclinical studies have shown temporal changes in the levels of oxygen of solid tumors during radiotherapy (10, 16–19). We propose that the appropriate schedule of fractions guided by tumor pO_2 could enhance therapeutic outcome. Assessment of tumor hypoxia by positron emission tomography (PET) has already shown a great promise in clinical applications (20–22). We have focused on the development of EPR oximetry, which can also provide repeated assessments of average tumor pO_2 with minimal perturbation to the microenvironment (23, 24). EPR oximetry has been used extensively for pO_2 measurements in animal models (10, 18, 25) and is now being developed for clinical applications (26, 27). Multisite EPR oximetry using magnetic field gradients has further expanded its *in vivo* application by allowing simultaneous pO_2 measurements at 2–4 sites in a tissue of interest (10, 18, 25, 28). In this study, we have investigated the effect of single hypofractionated radiation doses of less than 10 Gy on the ectopic 9L and C6 glioma pO_2 by multisite EPR oximetry. The delay in the tumor growth was determined with and without the subsequent fractionation being guided by glioma pO_2. Our results indicate that the pO_2 of C6 tumors increased significantly with irradiation of 4.8–9.3 Gy. However, no change in the pO_2 of the 9L tumors was observed. A significant decrease in the growth of C6 tumors was observed when the subsequent irradiation was scheduled at times of increase in pO_2. Therefore, the extent of increase in the pO_2 of the C6 tumors during radiotherapy was successfully used to identify responders and nonresponders, which had a significant difference in the tumor growth delay.

MATERIALS AND METHODS

Animals and Tumor Models

All animal procedures were in strict accordance with the NIH Guide for the Care and Use of Laboratory Animals and were approved by the Institutional Animal Care and Use Committee of Dartmouth Medical School (Geisel School of Medicine). The 9L gliomas have a sarcomatous appearance histologically and have been extensively used as a subcutaneous tumor model (29, 30). The C6 gliomas are classified as an astrocytoma with gene expression similar to that of human brain tumors (29, 30). The 9L and C6 tumors are syngeneic to the Fisher and Sprague-Dawley rats, respectively. These tumors were grown in male SCID mice (18–20 g) purchased from Charles River Laboratory (Wilmington, MA) and housed in the animal resource facility at Geisel School of Medicine.

Culture and Inoculation of 9L and C6 Glioma Cells

The 9L and C6 glioma cells were purchased from ATCC (Manassas, VA) and propagated in Dulbecco's Modified Eagle's medium with 4.5 g/L glucose, 1 m*M* sodium pyruvate, 10% FBS and 1% penicillin-streptomycin. When confluent, the cells were trypsinized and suspended in medium with no serum or additives. The procedure for tumor inoculation has been described previously (10, 18, 25). Briefly, subcutaneous tumors of 6–8 mm in length were obtained approximately 12–14 days after the injection of 100 μl cell suspension containing 4–5 × 10^5 cells in the left posterior flank of SCID mice.

Implantation of the Oximetry Probe

Lithium phathalocyanine (LiPc) crystals were synthesized in our laboratory and the physicochemical properties of LiPc crystals have been described previously (31). The LiPc crystals have a single sharp EPR line, the width of which is highly sensitive to pO_2. It has been shown that the EPR spectra reflect the average partial pressure of oxygen on the

surface of each LiPc aggregate and allows the measurements of tumor pO_2 using only a few crystals with a weight of approximately 30–50 μg. The volume of each LiPc aggregate is 0.09–0.15 mm^3. The procedure for LiPc injection was described previously (10, 18, 25). Briefly, mice were anesthetized with 1.5% isoflurane with 30% O_2, and two aggregates of the LiPc crystals were implanted at a depth of 2 mm and a distance of 4 mm into each tumor using 25-gauge needles. A pretreatment (baseline) pO_2 of the tumors was measured 24 h after LiPc implantation by multisite EPR oximetry.

Multisite EPR Oximetry

Assessment of tissue pO_2 at 2–4 sites both simultaneously and repeatedly by EPR oximetry (referred to as multisite EPR oximetry) has been used in animal models (10, 18, 25, 28). In these experiments, we have assessed pO_2 at two sites in each tumor using two implants of LiPc aggregates. The EPR oximetry was performed on an L-band (1,200 MHz) EPR spectrometer using a microwave bridge and an external loop resonator specially designed for *in vivo* experiments (32). A set of coils capable of generating a magnetic field gradient in the Z-direction with a magnitude up to 3.0 G/cm was used to separate the EPR spectra of the two implants in each tumor (18, 25, 33). The pO_2 measured from the two LiPc implants of each tumor were pooled to determine the average pO_2 of each tumor.

The spectrometer parameters were: incident microwave power, 2 mW; magnetic field center, 425 gauss; scan range, 2 gauss; modulation frequency, 24 kHz; modulation amplitude was one-third of the EPR line width with scan time of 10 s. The EPR line widths were converted to pO_2 using a calibration determined for each batch of LiPc crystals (18, 25, 31).

Experiment Protocol

The mice were assigned randomly into 5 groups for each glioma model: (A and B) control (sham-irradiated on day 1, $N_{9L} = 7$ and $N_{C6} = 7$); (C and D) single dose of 4.8 Gy on day 1 ($N_{9L} = 5$ and $N_{C6} = 7$); (E and F) single dose of 5.7 Gy on day 1 ($N_{9L} = 5$ and $N_{C6} = 9$); (G and H) single dose of 7.0 Gy on day 1 ($N_{9L} = 7$ and $N_{C6} = 7$); and (I and J) single dose of 9.3 Gy on day 1 ($N_{9L} = 5$ and $N_{C6} = 8$). The effect of subsequent irradiation was investigated when the C6 gliomas were oxygenated: (K) 4.8 Gy on day 1 and day 2, $N_{C6} = 24$. The results were also compared with standard fractionation and respective control: (L) 2.0 Gy × 5 ($N_{C6} = 7$) and (M) control (0 Gy, $N_{C6} = 11$). These groups are shown in Table 1.

For tumor pO_2 measurements, the mice were anesthetized (1.5% isoflurane, 30% O_2) and positioned between the poles of the EPR magnet. A baseline pO_2 was measured for 30 min (day 1) and then the animals were moved to the irradiator bed of a Varian Linear Accelerator (Clinac 2100C, 6 Mev, 6 × 6 cm applicator). The 6 × 6 cm lead applicator had a thickness of 15 mm with a gap (semicircle of 18 mm length and 9 mm radius) in the center to focus the radiation beam on the tumor. An additional lead shield (70 mm length, 60 mm width and 1.5 mm thickness) was used to expose the tumors and further minimize the irradiation of the adjoining normal tissue. The animals were kept anesthetized (1.5% isoflurane, 30% O_2) during irradiation. The hypofractionated doses were determined by a calculation based on the linear quadratic formula for cell survival to calculate the “standard equivalent dose (SED)” for planning hypofractionated stereotactic radiotherapy (34, 35). The fractions of 4.8 Gy × 10, 5.7 Gy × 8, 7 Gy × 6 and 9.3 Gy × 4 approximate the biological effect of a 70 Gy (35 fractions of 2 Gy each) dose plan for 9L and C6 tumors (36). The measurements of tumor pO_2 were repeated from day 2 to day 5 along with tumor volume measurements by a standard procedure (volume = $\pi/6 \times \text{length} \times \text{width}^2$) from day 1 to day 6. The tumor growth was also followed for up to 14 days to assess tumor growth delay in groups K, L and M.

Physiological Control and Histological Analysis

During EPR measurements, the body temperature of the animals was monitored using a rectal probe and was maintained at 37.0 ± 0.5° using a thermostatically controlled heated pad and a flow of warm air. The animals were kept warm by an electric heating pad during transportation to and from the irradiator. On day 6, the animals were euthanized, and tumors were removed, fixed and sectioned. Microscopic examination (H&E staining) of the tissue around the implanted LiPc deposits was performed to confirm its location in the tumor.

Statistical Analysis

A paired *t* test was used to determine the statistical significance of changes in pO_2 and tumor volume within the group, and an unpaired *t* test was used to determine the statistical significance between groups. The paired comparison reduces the animal-to-animal heterogeneity and eliminates differences of the baseline pO_2. The tumor growth delay was modeled by using an exponential mixed model (37, 38) on the log scale, and estimated by the linear mixed effects (LME) function in the statistical package S-Plus 6.1 (Insightful Inc., Seattle, WA). Assuming an exponential growth, the time to reach 4× the tumor volume of T4TV was computed as T4TV = ln4/a, where “a” is the rate of tumor volume growth obtained from LME. The standard error for T4TV was estimated using the delta method as described by Rice (39). The tests were two-sided, and a change with a $P < 0.05$ was considered statistically significant. This approach has been used previously to estimate tumor growth (40–42). All data are expressed as mean ± SEM and N is the total number of animals in each group.

RESULTS

Effect of Single-Dose Irradiation on Ectopic Glioma pO_2 and Growth

The average pO_2 of 9L and C6 tumors after single-dose irradiations with 4.8, 5.7, 7.0 and 9.3 Gy are shown in Figs. 1 and 2, respectively. The 9L tumors were hypoxic with a baseline pO_2 of 8.2–8.9 mmHg on day 1 (Fig. 1). The pO_2 of the 9L tumors declined with growth over days. Some of the individual 9L tumors showed an increase in tumor pO_2. However, no significant change in the average 9L tumor pO_2 in each group was observed with irradiation of 4.8–9.3 Gy.

The C6 tumors also were hypoxic with a baseline pO_2 of 5.4–7.1 mmHg on day 1 (Fig. 2). A significant increase in the pO_2 of C6 tumors was observed from day 2 to day 5 of irradiation with single doses of 4.8–9.3 Gy. However, the time to a significant increase in tumor pO_2 varied with different doses.

The baseline tumor volumes (day 1) of 9L and C6 tumors were similar between groups (Fig. 3). Irradiation with 4.8–9.3 Gy did not affect the growth of 9L tumors compared to the control group (Fig. 3b). However, the growth of the C6 gliomas were significantly reduced on day 3 to day 6 after single-dose irradiations with 4.8–9.3 Gy (Fig. 3a). No correlation between the baseline tumor pO_2 and tumor growth were observed in these experiments.

Effect of 4.8 Gy × 2 and 2 Gy × 5 on C6 Tumor pO_2 and Growth

The lowest dose that led to a significant increase in C6 tumor pO_2 on day 2 was 4.8 Gy. Therefore, a subsequent irradiation with 4.8 Gy (group K) was used to investigate the effect on C6 tumor pO_2 and growth (Fig. 4). A significant increase in the pO_2 of C6 tumor was observed from day 2 to day 4 when irradiated with 4.8 Gy on days 1 and 2. In contrast, no significant increase in the pO_2 occurred with irradiation of 2.0 Gy × 5 (Fig. 4, group L, gray diamond symbol).

No significant differences between the baseline tumor volume of the control and treatment groups were observed (Fig. 5). However, the tumor volume of the 4.8 Gy × 2 (group K) and 2.0 Gy × 5 (group L) significantly decreased from day 5 to day 14 compared to the control (group M). A significant difference in the tumor growth between groups K and L was observed only on day 5 and tumor growth was similar at later time points. The time to reach 4× tumor volume (T4TV) was 10.2 days for the control group, 13.1 and 14.9 days for groups K and L, respectively. The T4TV of group K (4.8 × 2) and L (2.0 Gy × 5) was significantly higher than for group M. However, no significant difference in the T4TV between K and L groups was evident.

To test the prognostic potential of glioma pO_2, the animals of group K were separated into subgroups based on the temporal changes in their pO_2: K1, C6 gliomas with increase in pO_2 on day 2 <50% of baseline (nonresponder), and K2, C6 gliomas with increase in pO_2 on day 2 ≥50% of baseline (responder) after 4.8 Gy. The numbers of tumors in the responder and nonresponder groups were 11 and 13, respectively. A significant difference in the tumor pO_2 from day 2 to day 5 and growth from day 3 to day 10 was evident between responder and nonresponder groups (Figs. 6 and 7). The T4TV of the responders (11.9 days, K2) was significantly greater than the nonresponders (8.3 days, K1) (Fig. 7, inset). These results indicate that 4.8 Gy irradiation of the oxygenated tumors (responders) on day 2 resulted in a significant growth inhibition compared to hypoxic tumors (nonresponders). Such analyses could not be carried out in group L (2 Gy × 5) due to no change in pO_2 during the irradiations.

Histological Analysis

Histological examination showed fibrotic cells around the LiPc aggregates in the 9L and C6 tumors after 1, 3 and 5 days of implantation (no irradiation group), respectively (Fig. 8). However, some blood cells and inflammatory cells were observed in the tumor sections. These observations represent a typical tissue environment in solid tumors and are unlikely to perturb the tissue pO_2 reported by LiPc implants in the tumors. In the normal tissue, we have seen negligible histological changes around LiPc implants (43–45).

DISCUSSION

The data reported here is the continuation of our systematic study to characterize the changes in tumor pO_2 after irradiation by EPR oximetry. We have previously reported the effect of a synthetic allosteric modifier of hemoglobin (efaproxiral), a vasodilator, benzyl nicotinate (BN), and carbogen inhalation on the RIF-1 tumor pO_2 with the goal to enhance tumor oxygenation and improve treatment efficacy by scheduling irradiations at times of increase in tumor pO_2 (10, 18, 25, 46). The results obtained here with ectopic 9L and C6 glioma indicate that these tumors are hypoxic with a pO_2 of <10 mmHg, consistent with our earlier observations (47, 48). Cerniglia *et al.* also has reported ectopic 9L glioma pO_2 of less than 8 mmHg in rats using a phosphorescence quenching method (49). Furthermore, a median pO_2 of 2 mmHg in the ectopic 9L glioma in the rats has also been observed by Teicher *et al.* (50, 51). In contrast, orthotopic 9L gliomas in the rats are well oxygenated (36). These results indicate a site specific effect on glioma pO_2. Indeed, Wallen *et al.* suggested a difference in the vasculature between orthotopic and ectopic 9L gliomas as a likely reason for the absence of hypoxia in orthotopic 9L gliomas (52).

The irradiation with single hypofractionated doses of less than 10 Gy did not affect the pO_2 of 9L tumors, while a significant increase in the C6 tumor pO_2 was observed. A significant increase in the oxygenation of LS174T human colon adenocarcinoma on irradiation with a total dose of more than 10 Gy has been observed by Znati *et al.* (53). An increase in SCC VII murine tumor pO_2 at 6–24 h after irradiation with 10, 15 or 20 Gy was observed by Fuji

et al. (54). We have also reported a significant increase in the pO_2 of RIF-1 tumors irradiated with 10 Gy (10). Several potential mechanisms have been suggested for the reoxygenation of tumors after irradiation such as reduced oxygen consumption by radiation-damaged cells (55), cell loss leading to tumor shrinkage (56), migration of hypoxic cells to oxygenated areas (57) and improved microcirculation (58).

We observed a significant decrease in the growth of C6 tumors after irradiation, which we did not observe with 9L tumors. This suggested that 9L tumor cells may be relatively radioresistant compared to C6 tumor cells. Indeed, others have shown that the surviving fractions after 2 Gy were indeed significantly higher (71%) for 9L versus 53% for C6 cells respectively (59). As stated above, we observed significant increase in the C6 tumor pO_2 and T4TV after irradiation with 4.8 Gy × 2 compared to the control. The T4TV for C6 tumors observed with the 4.8 Gy × 2 was similar to that of the 2 Gy × 5 group. Furthermore, the C6 tumors with an increase in pO_2 of more than 50% from the baseline had a significant increase in growth delay compared to those with pO_2 less than 50% from the baseline in the 4.8 Gy × 2 (K group). The observed increases in the pO_2 of the C6 tumors on day 2 to day 4 are consistent with previous reports (12, 60–62). Fukawa *et al.* has shown an increase in tumor pO_2 as late as day 3 in NFSa fibrosarcomas treated with 25 Gy (63). However, only a few investigators have described the temporal changes in tumor pO_2 during fractionated radiotherapy and how this could be used as a prognostic marker during radiotherapy. Our results indicate that the decrease in the C6 tumor growth with treatments of 4.8 Gy × 2 was dependent on the oxygenation status of the tumor after the first irradiation. These results suggest that the temporal changes in tumor pO_2 in such cases could indeed potentially be used to identify responders during radiotherapy. We anticipate that this approach could facilitate the design of better therapeutic approaches for nonresponding tumors.

In conclusion, our results demonstrate a glioma specific response to radiotherapy and a significant decrease in the C6 tumor growth when the fractionated radiations of 4.8 Gy × 2 were scheduled at times of increased pO_2. These results highlight the importance of tumor pO_2 assessment during fractionated radiotherapy and provide evidence that the temporal changes in tumor pO_2 can potentially be used to enhance as well as predict therapeutic response. Furthermore, these results also illustrate the ability of EPR oximetry, to make repetitive and noninvasive measurements of pO_2 from the same tumors during the course of therapy. EPR oximetry may prove very useful in individualizing the treatment of patients by following the response of tumor pO_2 during treatment. We have built clinical EPR spectrometers that will permit us to eventually extend this research into clinical trials (26, 27, 64). EPR oximetry is currently being used to follow the pO_2 of superficial tumors such as melanomas and sarcomas in patients undergoing chemoradiation (27). Implantable resonators are currently being pursued for repeated assessment of pO_2 in the tumors located at depths of more than 10 mm from the surface (26, 27, 64).

Acknowledgments

We thank Harriet St. Laurent and Kerry A. Tillson of Radiation Oncology, DHMC for assistance in the use of the radiation facility. This work was supported by NIH grant CA120919 to NK and used the facilities of the EPR Center.

REFERENCES

1. Bertout JA, Patel SA, Simon MC. The impact of O2 availability on human cancer. Nat Rev Cancer. 2008; 8(12):967–75. [PubMed: 18987634]
2. Hall, EJ. Radiobiology for the radiologist. 5th ed.. Lippincott Williams & Wilkins; Philadelphia: 2000. p. 91-111.

3. Vaupel P. Hypoxia and aggressive tumor phenotype: implications for therapy and prognosis. Oncologist. 2008; 13(Suppl 3):21–6. [PubMed: 18458121]
4. Vaupel P, Mayer A. Hypoxia in cancer: significance and impact on clinical outcome. Cancer Metast Rev. 2007; 26(2):225–39.
5. Weinmann M, Belka C, Plasswilm L. Tumour hypoxia: impact on biology, prognosis and treatment of solid malignant tumours. Onkologie. 2004; 27(1):83–90. [PubMed: 15007254]
6. Kim IH, Brown JM. Reoxygenation and rehypoxiation in the SCCVII mouse tumor. Int J Radiat Oncol Biol Phys. 1994; 29(3):493–7. [PubMed: 8005805]
7. Olive PL, Vikse CM, Durand RE. Hypoxic fractions measured in murine tumors and normal tissues using the comet assay. Int J Radiat Oncol Biol Phys. 1994; 29(3):487–91. [PubMed: 8005804]
8. Auberger T, Thurriegl B, Freude T, Weissfloch L, Senekowitsch-Schmidke R, Kneschaurek P, et al. Oxygen tension in transplanted mouse osteosarcomas during fractionated high-LET and low-LET radiotherapy–predictive aspects for choosing beam quality? Strahlenther Onkol. 1999; 175(Suppl 2):52–6. [PubMed: 10394398]
9. Cooper RA, West CM, Logue JP, Davidson SE, Miller A, Roberts S, et al. Changes in oxygenation during radiotherapy in carcinoma of the cervix. Int J Radiat Oncol Biol Phys. 1999; 45(1):119–26. [PubMed: 10477015]
10. Hou H, Lariviere JP, Demidenko E, Gladstone D, Swartz H, Khan N. Repeated tumor pO(2) measurements by multi-site EPR oximetry as a prognostic marker for enhanced therapeutic efficacy of fractionated radiotherapy. Radiother Oncol. 2009; 91:126–31. [PubMed: 19013657]
11. Lyng H, Tanum G, Evensen JF, Rofstad EK. Changes in oxygen tension during radiotherapy of head and neck tumours. Acta Oncol. 1999; 38(8):1037–42. [PubMed: 10665759]
12. O'Hara JA, Goda F, Demidenko E, Swartz HM. Effect on regrowth delay in a murine tumor of scheduling split-dose irradiation based on direct pO2 measurements by electron paramagnetic resonance oximetry. Radiat Res. 1998; 150(5):549–56. [PubMed: 9806597]
13. Wachsberger PR, Burd R, Marero N, Daskalakis C, Ryan A, McCue P, et al. Effect of the tumor vascular-damaging agent, ZD6126, on the radioresponse of U87 glioblastoma. Clin Cancer Res. 2005; 11(2 Pt 1):835–42. [PubMed: 15701874]
14. Lally BE, Rockwell S, Fischer DB, Collingridge DR, Piepmeier JM, Knisely JP. The interactions of polarographic measurements of oxygen tension and histological grade in human glioma. Cancer J. 2006; 12(6):461–6. [PubMed: 17207315]
15. Raleigh JA, Dewhirst MW, Thrall DE. Measuring tumor hypoxia. Semin Radiat Oncol. 1996; 6(1): 37–45. [PubMed: 10717160]
16. Toma-Dasu I, Dasu A, Karlsson M. The relationship between temporal variation of hypoxia, polarographic measurements and predictions of tumour response to radiation. Phys Med Biol. 2004; 49(19):4463–75. [PubMed: 15552411]
17. Ljungkvist AS, Bussink J, Kaanders JH, Wiedenmann NE, Vlasman R, van der Kogel AJ. Dynamics of hypoxia, proliferation and apoptosis after irradiation in a murine tumor model. Radiat Res. 2006; 165(3):326–36. [PubMed: 16494521]
18. Hou H, Abramovic Z, Lariviere JP, Sentjurc M, Swartz H, Khan N. Effect of a topical vasodilator on tumor hypoxia and tumor oxygen guided radiotherapy using EPR oximetry. Radiat Res. 2010; 173(5):651–8. [PubMed: 20426665]
19. Fokas E, Hanze J, Kamlah F, Eul BG, Lang N, Keil B, et al. Irradiation-dependent effects on tumor perfusion and endogenous and exogenous hypoxia markers in an A549 xenograft model. Int J Radiat Oncol Biol Phys. 2010; 77(5):1500–8. [PubMed: 20637978]
20. Mortensen LS, Johansen J, Kallehauge J, Primdahl H, Busk M, Lassen P, et al. FAZA PET/CT hypoxia imaging in patients with squamous cell carcinoma of the head and neck treated with radiotherapy: Results from the DAHANCA 24 trial. Radiother Oncol. 2012; 105(1):14–20. [PubMed: 23083497]
21. Gaertner FC, Souvatzoglou M, Brix G, Beer AJ. Imaging of hypoxia using PET and MRI. Curr Pharm Biotechnol. 2012; 13(4):552–70. [PubMed: 22214501]
22. Carlin S, Humm JL. PET of hypoxia: current and future perspectives. J Nucl Med. 2012; 53(8): 1171–4. [PubMed: 22789676]

23. Bratasz A, Pandian RP, Deng Y, Petryakov S, Grecula JC, Gupta N, et al. In vivo imaging of changes in tumor oxygenation during growth and after treatment. Magn Reson Med. 2007; 57(5): 950–9. [PubMed: 17457861]
24. Elas M, Bell R, Hleihel D, Barth ED, McFaul C, Haney CR, et al. Electron paramagnetic resonance oxygen image hypoxic fraction plus radiation dose strongly correlates with tumor cure in FSa fibrosarcomas. Int J Radiat Oncol Biol Phys. 2008; 71(2):542–9. [PubMed: 18474313]
25. Hou H, Dong R, Lariviere JP, Mupparaju SP, Swartz HM, Khan N. Synergistic combination of hyperoxygenation and radiotherapy by repeated assessments of tumor pO(2) with EPR oximetry. J Radiat Res (Tokyo). 2011; 52(5):568–574. [PubMed: 21799293]
26. Khan N, Williams BB, Hou H, Li H, Swartz HM. Repetitive tissue pO2 measurements by electron paramagnetic resonance oximetry: current status and future potential for experimental and clinical studies. Antioxid Redox Signal. 2007; 9:1169–82. [PubMed: 17536960]
27. Williams BB, Khan N, Zaki B, Hartford A, Ernstoff MS, Swartz HM. Clinical electron paramagnetic resonance (EPR) oximetry using India ink. Adv Exp Med Biol. 2010; 662:149–56. [PubMed: 20204785]
28. Williams BB, Hou H, Grinberg OY, Demidenko E, Swartz HM. High spatial resolution multisite EPR oximetry of transient focal cerebral ischemia in the rat. Antioxid Redox Signal. 2007; 9(10): 1691–8. [PubMed: 17678442]
29. Barth RF, Kaur B. Rat brain tumor models in experimental neurooncology: the C6, 9L, T9, RG2, F98, BT4C, RT-2 and CNS-1 gliomas. J Neurooncol. 2009; 94(3):299–312. [PubMed: 19381449]
30. Dai C, Holland EC. Glioma models. Biochim Biophys Acta. 2001; 1551(1):M19–27. [PubMed: 11553418]
31. Liu KJ, Gast P, Moussavi M, Norby SW, Vahidi N, Walczak T, et al. Lithium phathalocyanine: a probe for electron paramagnetic resonance oximetry in viable biological systems. Proc Natl Acad Sci U S A. 1993; 90(12):5438–42. [PubMed: 8390665]
32. Swartz HM, Walczak T. Developing in vivo EPR oximetry for clinical use. Adv Exp Med Biol. 1998; 454:243–52. [PubMed: 9889898]
33. Smirnov AI, Norby SW, Clarkson RB, Walczak T, Swartz HM. Simultaneous multi-site EPR spectroscopy in vivo. Magn Reson Med. 1993; 30(2):213–20. [PubMed: 8396190]
34. Dale RG, Jones B, Sinclair JA. Dose equivalents of tumour repopulation during radiotherapy: the potential for confusion. Br J Radiol. 2000; 73(872):892–4. [PubMed: 11026867]
35. Denekamp J, Waites T, Fowler JF. Predicting realistic RBE values for clinically relevant radiotherapy schedules. Int J Radiat Biol. 1997; 71(6):681–94. [PubMed: 9246183]
36. Khan N, Li H, Hou H, Lariviere JP, Gladstone DJ, Demidenko E, et al. Tissue pO2 of orthotopic 9L and C6 gliomas and tumor-specific response to radiotherapy and hyperoxygenation. Int J Radiat Oncol Biol Phys. 2009; 73(3):878–85. [PubMed: 19136221]
37. Demidenko, E. Mixed models: theory and applications. Wiley; New York: 2004.
38. Demidenko E. Three endpoints of in vivo tumour radiobiology and their statistical estimation. Int J Radiat Biol. 2010; 86(2):164–73. [PubMed: 20148701]
39. Rice, J. Mathematical statistics and data analysis. Duxbury Press; Belmont, CA: 1995.
40. Begg, AC. Principles and practices of the tumor growth delay assay.. In: Kallman, RF., editor. Rodent tumor models in experimental cancer therapy. McGraw-Hill; New York: 1987. p. 114-21.
41. Pogue BW, O'Hara JA, Demidenko E, Wilmot CM, Goodwin IA, Chen B, et al. Photodynamic therapy with verteporfin in the radiation-induced fibrosarcoma-1 tumor causes enhanced radiation sensitivity. Cancer Res. 2003; 63(5):1025–33. [PubMed: 12615718]
42. Tubiana, M.; Dutreix, J.; Wambersie, A. Introduction to radiology. Taylor & Francis; London: 1990.
43. Ilangovan G, Li H, Zweier JL, Krishna MC, Mitchell JB, Kuppusamy P. In vivo measurement of regional oxygenation and imaging of redox status in RIF-1 murine tumor: effect of carbogen-breathing. Magn Reson Med. 2002; 48(4):723–30. [PubMed: 12353291]
44. Hou H, Dong R, Li H, Williams B, Lariviere JP, Hekmatyar SK, et al. Dynamic changes in oxygenation of intracranial tumor and contralateral brain during tumor growth and carbogen breathing: a multisite EPR oximetry with implantable resonators. J Magn Reson. 2012; 214(1):22–8. [PubMed: 22033225]

45. Dunn JF, Swartz HM. In vivo electron paramagnetic resonance oximetry with particulate materials. Methods. 2003; 30(2):159–66. [PubMed: 12725782]
46. Hou H, Khan N, Grinberg OY, Yu H, Grinberg SA, Lu S, et al. The effects of Efaproxyn (efaproxiral) on subcutaneous RIF-1 tumor oxygenation and enhancement of radiotherapy-mediated inhibition of tumor growth in mice. Radiat Res. 2007; 168(2):218–25. [PubMed: 17638413]
47. Mupparaju S, Hou H, Lariviere JP, Swartz H, Jounaidi Y, Khan N. Repeated tumor oximetry to identify therapeutic window during metronomic cyclophosphamide treatment of 9L gliomas. Oncol Rep. 2011; 26(1):281–6. [PubMed: 21503586]
48. Mupparaju S, Hou H, Lariviere JP, Swartz HM, Khan N. Tumor pO as a surrogate marker to identify therapeutic window during metronomic chemotherapy of 9L gliomas. Adv Exp Med Biol. 2011; 701:107–13. [PubMed: 21445776]
49. Cerniglia GJ, Wilson DF, Pawlowski M, Vinogradov S, Biaglow J. Intravascular oxygen distribution in subcutaneous 9L tumors and radiation sensitivity. J Appl Physiol. 1997; 82(6): 1939–45. [PubMed: 9173962]
50. Teicher BA, Herman TS, Rose CM. Effect of Fluosol-DA on the response of intracranial 9L tumors to X rays and BCNU. Int J Radiat Oncol Biol Phys. 1988; 15(5):1187–92. [PubMed: 3141321]
51. Teicher BA, Holden SA, Ara G, Dupuis NP, Liu F, Yuan J, et al. Influence of an anti-angiogenic treatment on 9L gliosarcoma: oxygenation and response to cytotoxic therapy. Int J Cancer. 1995; 61(5):732–7. [PubMed: 7768649]
52. Wallen CA, Michaelson SM, Wheeler KT. Evidence for an unconventional radiosensitivity of rat 9L subcutaneous tumors. Radiat Res. 1980; 84(3):529–41. [PubMed: 7454994]
53. Znati CA, Rosenstein M, Boucher Y, Epperly MW, Bloomer WD, Jain RK. Effect of radiation on interstitial fluid pressure and oxygenation in a human tumor xenograft. Cancer Res. 1996; 56(5): 964–68. [PubMed: 8640786]
54. Fujii H, Sakata K, Katsumata Y, Sato R, Kinouchi M, Someya M, et al. Tissue oxygenation in a murine SCC VII tumor after X-ray irradiation as determined by EPR spectroscopy. Radiother Oncol. 2008; 86(3):354–60. [PubMed: 18077029]
55. Zhao D, Constantinescu A, Chang CH, Hahn EW, Mason RP. Correlation of tumor oxygen dynamics with radiation response of the dunning prostate R3327-HI tumor. Radiat Res. 2003; 159(5):621–31. [PubMed: 12710873]
56. Kallman RF. The phenomenon of reoxygenation and its implications for fractionated radiotherapy. Radiology. 1972; 105(1):135–42. [PubMed: 4506641]
57. Brown JM. Evidence for acutely hypoxic cells in mouse tumours, and a possible mechanism of reoxygenation. Br J Radiol. 1979; 52(620):650–6. [PubMed: 486895]
58. Yeh KA, Biade S, Lanciano RM, Brown DQ, Fenning MC, Babb JS, et al. Polarographic needle electrode measurements of oxygen in rat prostate carcinomas: accuracy and reproducibility. Int J Radiat Oncol Biol Phys. 1995; 33(1):111–8. [PubMed: 7642408]
59. Bencokova Z, Pauron L, Devic C, Joubert A, Gastaldo J, Massart C, et al. Molecular and cellular response of the most extensively used rodent glioma models to radiation and/or cisplatin. J Neurooncol. 2008; 86(1):13–21. [PubMed: 17611717]
60. Ando K, Koike S, Ohira C, Chen YJ, Nojima K, Ando S, et al. Accelerated reoxygenation of a murine fibrosarcoma after carbonion radiation. Int J Radiat Biol. 1999; 75(4):505–12. [PubMed: 10331856]
61. Koutcher JA, Alfieri AA, Devitt ML, Rhee JG, Kornblith AB, Mahmood U, et al. Quantitative changes in tumor metabolism, partial pressure of oxygen, and radiobiological oxygenation status postradiation. Cancer Res. 1992; 52(17):4620–7. [PubMed: 1511430]
62. Vaupel P, Frinak S, O'Hara M. Direct measurement of reoxygenation in malignant mammary tumors after a single large dose of irradiation. Adv Exp Med Biol. 1984; 180:773–82. [PubMed: 6534148]
63. Fukawa T, Takematsu K, Oka K, Koike S, Ando K, Kobayashi H, et al. Differences in pO2 peaks of a murine fibrosarcoma between carbon-ion and X-ray irradiation. J Radiat Res (Tokyo). 2004; 45(2):303–8. [PubMed: 15304974]

64. Swartz HKN, Buckey J, Comi R, Gould L, Grinberg O, Hartford A, et al. Clinical applications of EPR: overview and perspectives. NMR Biomed. 2004; 17(5):335–51. [PubMed: 15366033]

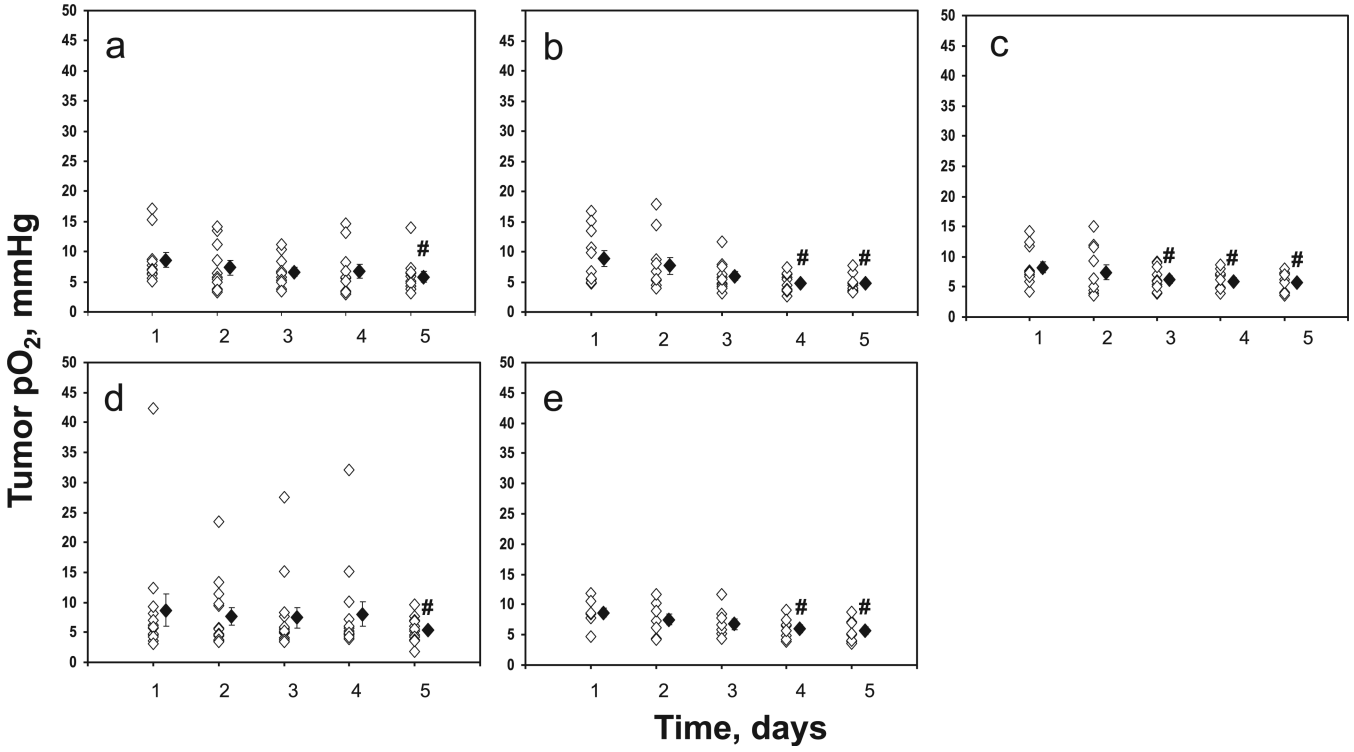

FIG. 1.

The ectopic 9L glioma pO_2 over days in the groups treated with single doses, panel a: control, 0 Gy, N = 7; panel b: 4.8 Gy, N = 5; panel c: 5.7 Gy, N = 5; panel d: 7.0 Gy, N = 7; panel e: 9.3 Gy, N = 5. (◇) Represents the tumor pO_2 recorded from each EPR probe and (◆) represents the mean tumor pO_2 within 20 min in the same day. Mean ± SEM, $^{\#}P < 0.05$ vs. baseline tumor pO_2 (day 1).

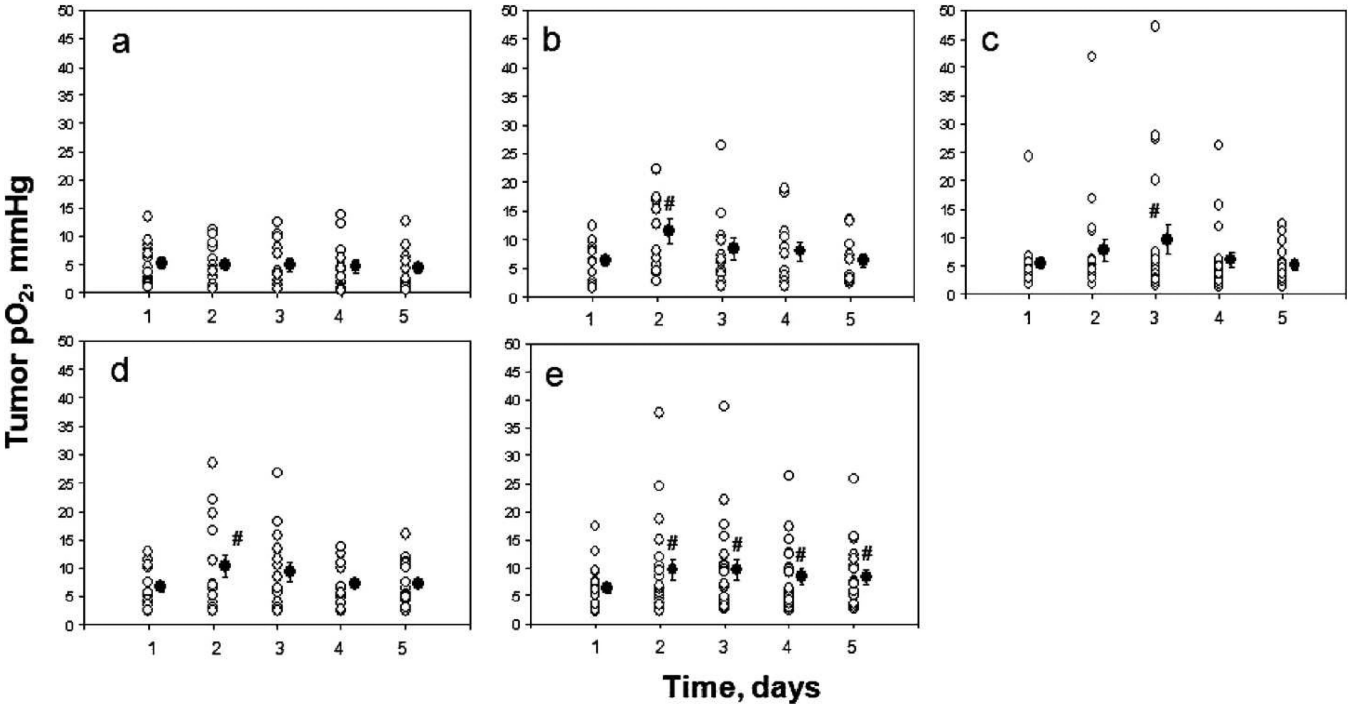

FIG. 2.

The C6 glioma pO_2 over days in the groups treated, panel a: control, 0 Gy, N = 7; panel b: 4.8 Gy, N = 7; panel c: 5.7 Gy, N = 9; panel d: 7.0 Gy, N = 7; panel e: 9.3 Gy, N = 8. (○) Represents the tumor pO_2 recorded from each EPR probe and (●) represent the mean tumor pO_2 within 20 min in the same day. Mean ± SEM, $^{\#}P < 0.05$ vs. baseline tumor pO_2 (day 1).

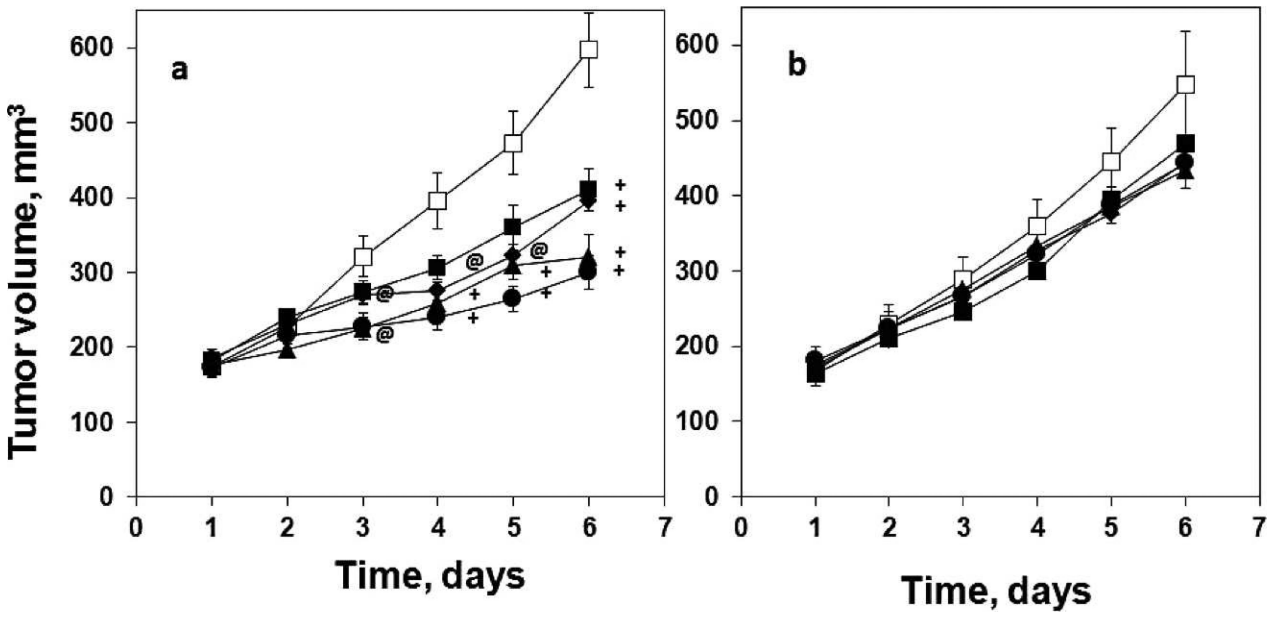

FIG. 3.

The growth of C6 glioma (panel a) and 9L glioma (panel b) over days in the groups treated with (□): control, 0 Gy; (■): 4.8 Gy; (◆): 5.7 Gy; (▲): 7.0 Gy; (●): 9.3 Gy. Mean ± SEM, $^{@}P < 0.05$, $^{+}P < 0.01$ vs. control group at the same time point.

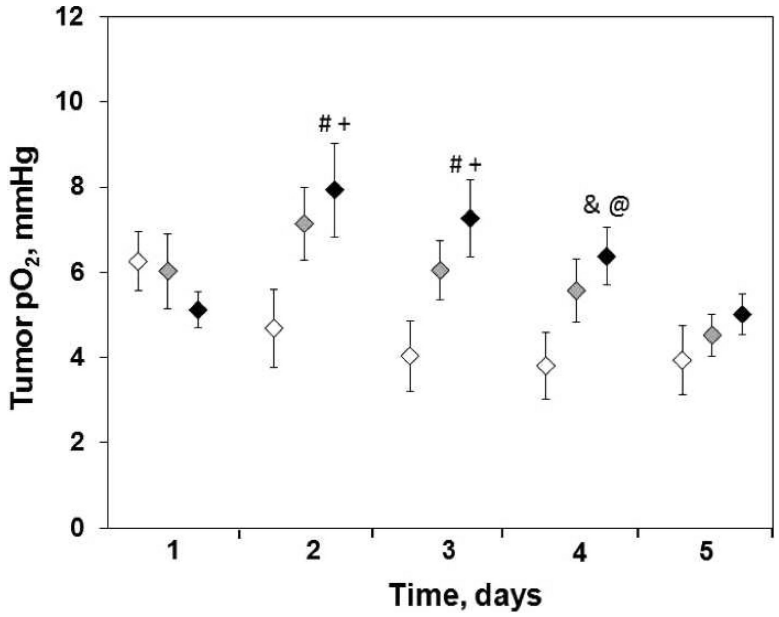

FIG. 4.

Temporal changes in the average C6 glioma pO_2 before and after irradiation. (white symbol) 0 Gy (control, N = 11), (black symbol) 4.8 Gy × 2 (day 1, day 2, N = 24) and (gray symbol) 2 Gy × 5 (day 1 to day 5, N = 7). Mean ± SEM, $^{\#}P < 0.05$, $^{\&}P < 0.01$, compared with the baseline pO_2 of the same group; $^{@}P < 0.05$, $^{+}P < 0.01$, compared with the pO_2 of control group on the same day.

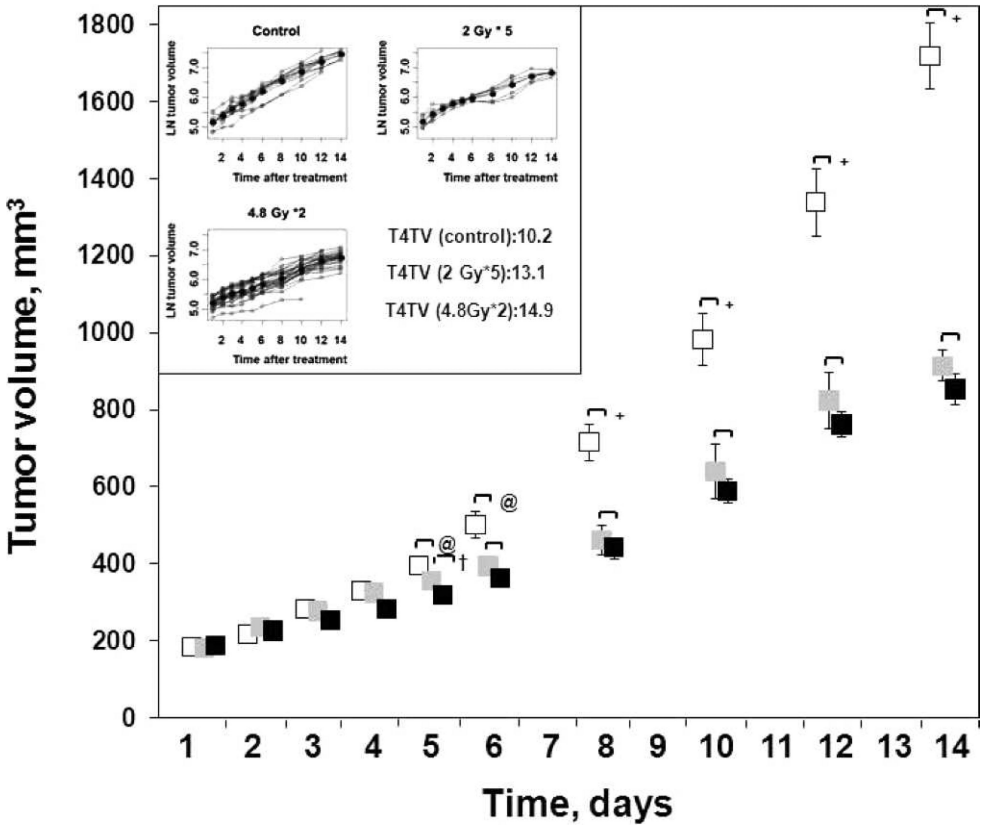

FIG. 5.

The changes in the C6 glioma growth in (white symbol) 0 Gy (M, N = 11), (black symbol) 4.8 Gy ×; 2 (K, N = 24) and (gray symbol) 2 Gy × 5 (L, N = 7) groups. Inset: Days to reach 4× the original tumor volume (T4TV) of groups M, K and L. The line in bold represents the mean data obtained from individual values on each day. Mean ± SEM, $^{@}P < 0.05$, $^{+}P < 0.01$, compared with the control group; $^{\dagger}P < 0.05$, compared with group L.

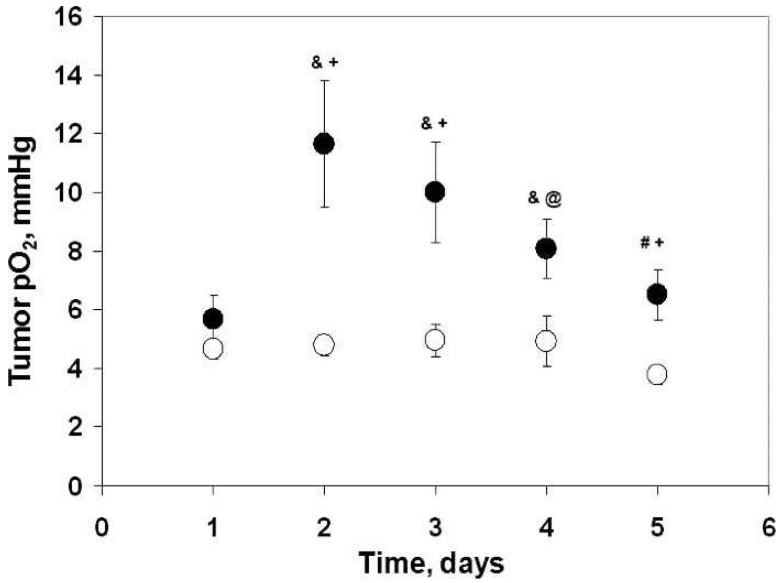

FIG. 6.

The C6 glioma pO_2 over days: (●) responders (K2, pO_2 on day 2 ≥50% of baseline, N = 11); (○) nonresponders (K1, pO_2 on day 2 <50 % of baseline, N = 13). Mean ± SEM, $^{\#}P < 0.05$, $^{\&}P < 0.01$, compared with the baseline pO_2 in the same group; $^{@}P < 0.05$, $^{+}P < 0.01$, compared with the glioma pO_2 of nonresponders on the same day.

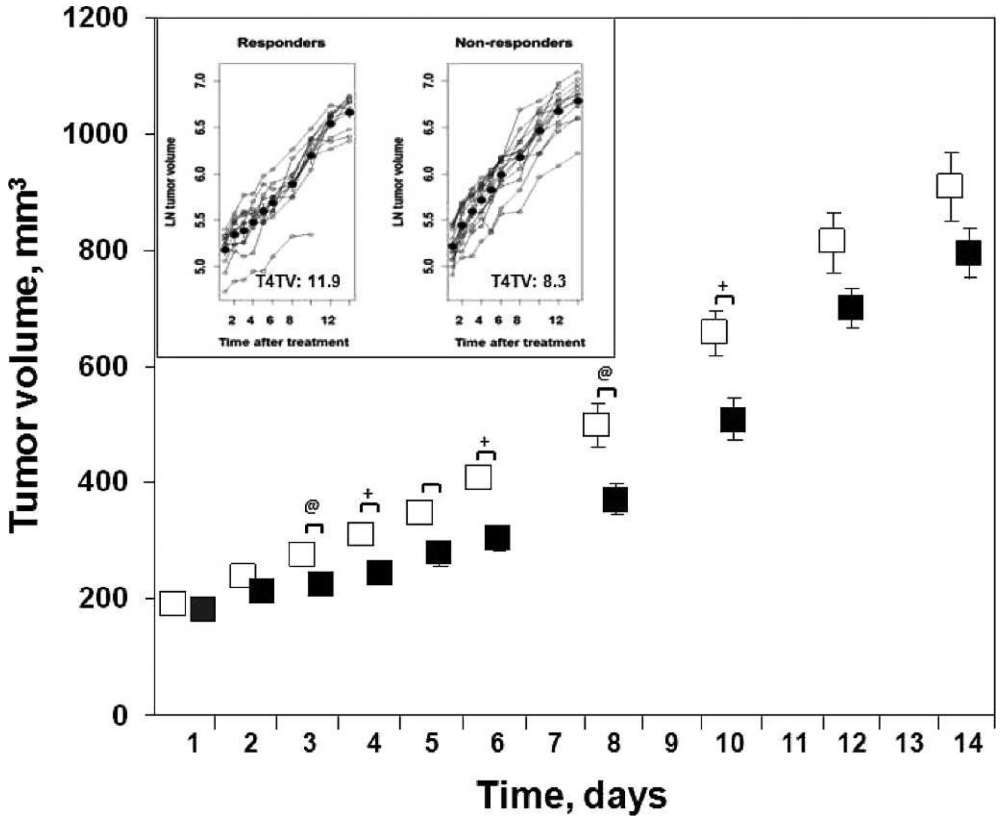

FIG. 7.

The C6 glioma growth over days: (■) responders (K2, pO_2 on day 2 ≥50% of baseline, N 11); (□) nonresponders (K1, pO_2 on day 2 <50% of baseline, N = 13). Inset: Number of days to reach 4× of baseline tumor volume (T4TV) of responders and nonresponders. The line in bold represents the mean data obtained from individual values at each time point. Mean ± SEM, $^{@}P < 0.05$, $^{+}P < 0.01$, compared with the nonresponders.

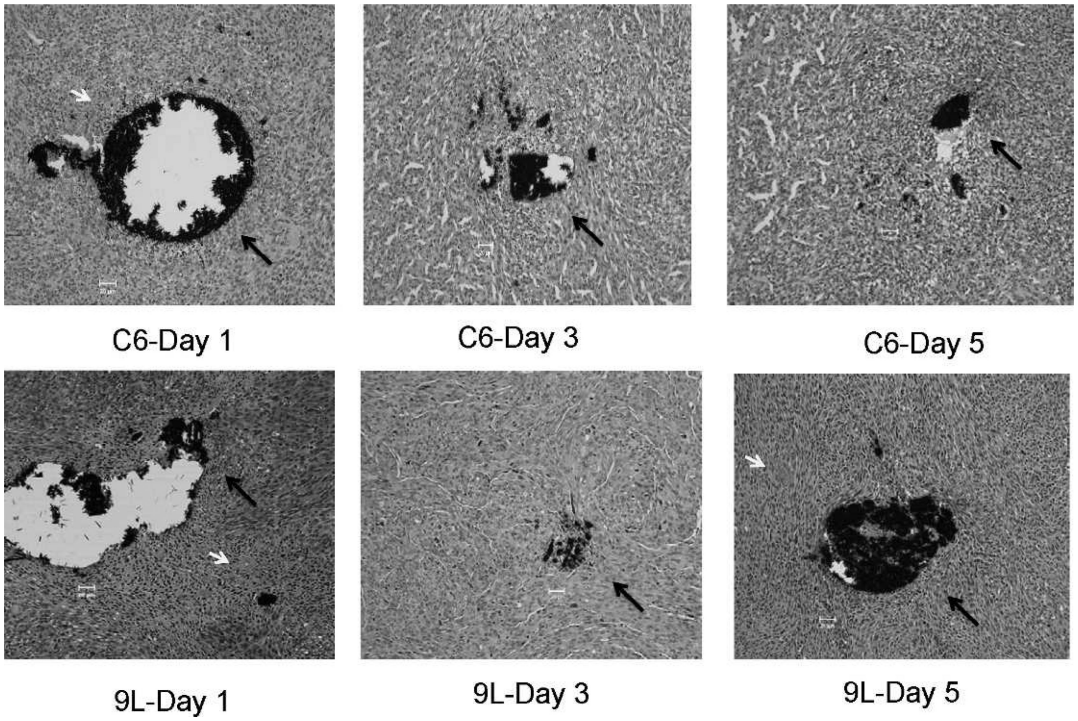

FIG. 8.

H&E stained sections of the C6 and 9L tumors obtained from the control mice on different days after LiPc implantation. The LiPc crystals (black color) are indicated by long black arrows and blood cells are indicated by short white arrows. The thickness of each section is 5 μm. Magnification: 20×.

TABLE 1

The Number of 9L and C6 Groups with Radiation Dose Used in the Study

Groups	Tumor types	Doses (Gy)	N
A	9L	0	7
B	C6	0	7
C	9L	4.8	5
D	C6	4.8	7
E	9L	5.7	5
F	C6	5.7	9
G	9L	7.0	7
H	C6	7.0	7
I	9L	9.3	5
J	C6	9.3	8
K	C6	4.8 × 2	24
L	C6	2.0 × 5	7
M	C6	0	11